HHS Public Access

Author manuscript

Adv Healthc Mater. Author manuscript; available in PMC 2021 July 01.

Published in final edited form as:

Adv Healthc Mater. 2020 July ; 9(14): e2000200. doi:10.1002/adhm.202000200.

Controlling the Release of Neurotrophin-3 and Chondroitinase ABC Enhances the Efficacy of Nerve Guidance Conduits

Dr. Anthony Donsante[#],
Department of Neurosurgery, Emory University, Atlanta, GA 30322, USA

Kelly M. Poth,
Department of Neurosurgery, Emory University, Atlanta, GA 30322, USA

Nathan S. Hardcastle,
Department of Neurosurgery, Emory University, Atlanta, GA 30322, USA

Bruna Diniz,
Department of Neurosurgery, Emory University, Atlanta, GA 30322, USA

Dr. Deirdre M. O'Connor,
Department of Neurosurgery, Emory University, Atlanta, GA 30322, USA

Prof. Nicholas M. Boulis,
Department of Neurosurgery, Emory University, Atlanta, GA 30322, USA

Dr. Jiajia Xue[#],
The Wallace H. Coulter Department of Biomedical Engineering, Georgia Institute of Technology and Emory University, Atlanta, GA 30332, USA

Prof. Younan Xia
The Wallace H. Coulter Department of Biomedical Engineering, Georgia Institute of Technology and Emory University, Atlanta, GA 30332, USA

School of Chemistry and Biochemistry, Georgia Institute of Technology, Atlanta, Georgia 30332, USA

Abstract

Nerve guidance conduits (NGCs) have the potential to replace autografts in repairing peripheral nerve injuries, but their efficacy still needs to be improved. The efficacy of NGCs may be augmented by neurotrophic factors that promote axon growth and by enzymes capable of degrading molecules that inhibit axon growth. In the current study, we constructed two types of NGCs loaded with factors (both neurotrophin-3 and chondroitinase ABC) and examined their abilities to repair an 8-mm gap in the rat sciatic nerve. The factors were encapsulated in microparticles made of a phase-change material (PCM) or collagen and then sandwiched between two layers of electrospun fibers. The use of PCM allowed us to achieve pulsed release of the

anthony.donsante@emory.edu (Donsante), younan.xia@bme.gatech.edu (Xia), and nboulis@emory.edu (Boulis).
[#]These two authors contributed equally to this work.

Supporting Information
Supporting Information is available from the Wiley Online Library or from the author.

factors upon irradiation with a near-infrared laser. The use of collagen enabled slow, continuous release *via* diffusion. The efficacy was evaluated by measuring compound muscle action potentials (CMAP) in the gastrocnemius muscle and analyzing the nerve histology. Continuous release of the factors from collagen resulted in enhanced CMAP amplitude and increased axon counts in the distal nerve relative to the plain conduit. In contrast, pulsed release of the same factors from PCM showed a markedly adverse impact on the efficacy, possibly by inhibiting axon growth.

Table of contents entry

Minding the release: Nerve guidance conduits are constructed using electrospun fibers and microparticles loaded with biological factors. The efficacy of the conduits for peripheral nerve repair in a rat model can be enhanced by the factors, but they have to be released slowly and continuously rather than in a pulsed pattern.

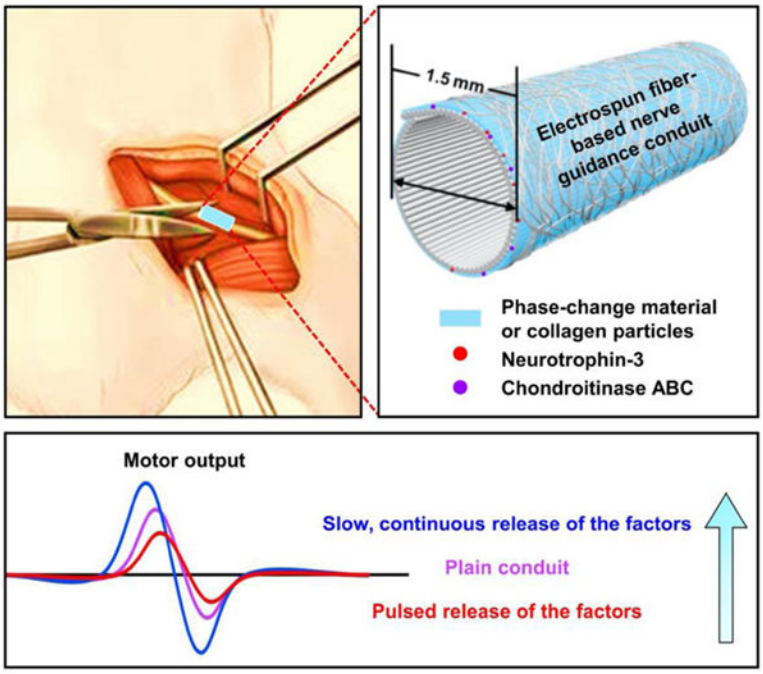

Keywords

peripheral nerve repair; nerve guidance conduit; neurotrophin-3; condroitinase ABC; controlled release

1. Introduction

Peripheral nerve injury is a widespread problem that results in neuropathy and motor deficits for millions of people every year.[1] Long gaps in thick nerves are difficult to treat. They cannot be repaired *via* direct anastomosis because tension on the recovering nerve can slow and diminish healing.[2] Although some treatments can facilitate nerve regrowth, functional recovery is usually limited.[3] The effectiveness of treatment is dependent on the amount of nerve that is damaged and the timing of repair after the initial injury. The current standard

for large-gap peripheral nerve repair is based on autologous grafts.[4] This treatment involves harvesting a healthy sensory nerve to replace the damaged portion of a motor nerve. The procedure can result in pain, loss of feeling, and neuroma formation in the areas associated with the donor nerves. Although autografts are considered the gold standard for peripheral nerve repair, only 40−50% of the patients regain function.[5] A large portion of current research focuses on the development of nerve guidance conduits (NGCs) to replace autografts. NGCs facilitate nerve regrowth across a gap by limiting the directions that axons can grow and perhaps by concentrating neurotrophic factors and protecting axons from scar tissue formation.[6] There are NGCs that are currently approved for clinical use, but they provide only moderate recovery for small gaps narrower than 15−20 mm.[7]

The therapeutic potential of NGCs may be enhanced with the addition of proteins or drugs that promote growth and survival of motor neurons and their axons. For example, many neurotrophic factors can enhance neurite outgrowth. These factors are biologically active at low concentrations and present within the nerve following nerve injury, making them obvious choices to augment the healing capacity of NCGs. Many factors have been tested with NCGs at different levels of success, including neurotrophin-3 (NT-3),[8] brain-derived neurotropic factor,[8a] glial-derived neurotrophic factor,[9] ciliary neurotrophic factor,[10] and vascular endothelial growth factor.[11] The effect of NT-3 on motor axon regeneration and restoration of motor function has not been extensively studied, even though motor neurons express a receptor for NT-3[12] and NT-3 is the predominant neurotrophin expressed by adult muscle.[13] Exogenous NT-3 can improve motor neuron conduction velocity following axotomy.[14] In addition, NT-3 enhances Schwann cell migration,[15] a property that could be useful during axon regeneration through an acellular NGC. It has also been shown that NT-3 is essential to the survival of mature Schwann cells, especially in the absence of healthy axons.[16] NT-3 has been shown to increase myelinated axons[8b] and increase muscle fiber recovery following nerve injury,[17] but it is not clear if the outcomes observed in these studies were due to the direct effect of NT-3 on motor axons. These tantalizing hints suggest that NT-3 can be useful in nerve gap repair involving NGCs.

Chondroitin sulfate proteoglycans (CSPGs) represent a class of potent axonal-regeneration inhibitors. They are a component of the basal laminae that forms a tubular extracellular matrix around each axon and its supporting Schwann cells.[18] Following peripheral nerve injury, scarring occurs and CSPGs are upregulated.[19] During the repair of a transected nerve, the increases in scarring and CSPGs in the distal stump adversely impact nerve regeneration by causing disorganization and misdirection of axon growth leading to reduced numbers of axons entering distal nerve segment and a poorer outcome in motor function.[20] In mice, the scarring that occurs following nerve injury can be altered through genetic manipulation: knocking out the mannose-6-phosphate receptor reduces scarring while knocking out IL-6 and IL-10 increases it.[21] In a mouse model of nerve transection, reducing scar formation improved compound action potentials, conduction velocity, and myelinated axon counts for augmentation in recovery.[21] These results suggest that altering the deposition of CSPGs in the distal nerve stump can enhance nerve repair. In addition to the scarring that occurs within the nerve, a foreign body reaction against the conduit might also contribute to the deposition of CSPGs on its surface, further inhibiting axonal growth across the gap.[22] Despite the success in mouse experiment, it remains impractical to

manipulate the genetics of a patient's nerve. Alternatively, an enzyme such as chondroitinase ABC (ChABC) can be delivered to help degrade inhibitory CSPGs.[19a,23] To this end, controlled release of ChABC from an NGC may increase its efficacy by eliminating inhibitory CSPGs within the conduit and in the distal stump, leading to improved repair of the nerve.

NGCs based on electrospun fibers have shown great promise in promoting peripheral nerve repair.[24] To this end, synthetic polymers, natural polymers, or mixtures of them have all been explored to construct NGCs for the repair of peripheral nerve injury,[24] with notable examples including polycaprolactone (PCL), poly(lactic-*co*-glycolic acid), collagen, and silk fibroin, as well as a mixture of poly(*L*-lactic acid-*co*-ε-caprolactone) and silk fibroin. As a semi-crystalline polyester, PCL has a slower biodegradation rate than all other polymers used for constructing NGCs, making it suitable for long-term studies with large animal models.[25] The NGCs typically involved the use of uniaxially aligned fibers for leveraging the contact guidance to promote neurite extension along the direction of alignment and thereby increase the lengths of the neurites relative to the case of random fibers.[26] Adding biological effectors such as growth factors and enzymes into the fiber-based NGCs can further augment axon growth while preventing inhibitory mechanisms. In our previous study, we found that the factors could be triggered to release in a controlled, step-wise manner with preserved bioactivity upon irradiation with a near-infrared (NIR) laser by encapsulating them in a thermosensitive material such as phase-change material (PCM).[27] The PCM could be formulated from a eutectic mixture of lauric acid and stearic acid to give a constant melting temperature and a large latent heat. Compared with other types of thermosensitive materials made of polymers, these two fatty acids occur naturally, rendering them good biocompatibility and biodegradability.[27a] Specifically, when PCM particles loaded with NT-3 were sandwiched between two layers of electrospun fibers, neurite extension was augmented upon laser irradiation.[27c] We suspect that both NT-3 and ChABC can be co-encapsulated in the PCM to trigger their release upon irradiation with a laser. Alternatively, these two factors can be released continuously in a slow, steady manner through encapsulation in polymeric particles.[28] Here, we evaluate and compare the efficacies of NGCs based on electrospun fibers when they are integrated with both NT-3 and ChABC using two different means of release for nerve injury repair in a rat model.

2. Results and Discussion

2.1 Controlling the Release of NT-3 and ChABC from the NGCs

We fabricated three types of NGCs from electrospun fibers: plain conduit, conduit containing PCM particles for the heat-released factors (NGC+hr-factors), and conduit containing collagen particles for the continuously-released factors (NGC+cr-factors). The inner diameter of the conduits was about 1.5 mm. The plain conduit was fabricated by rolling up a bilayer mat of electrospun PCL fibers, with the inner layer comprised of uniaxially aligned fibers and the outer layer comprised of random fibers.[24a] The boundary of the conduit was then sealed using the same PCL solution used for electrospinning. Figure S1 shows a scanning electron microscopy (SEM) image of the cross-section of the plain conduit. In this image, the cross-section of the conduit did not appear as a circular ring

because of the deformation during sample preparation. Most of the fibers in the inner wall were perpendicular to the image, indicating their uniaxial alignment along the conduit. In comparison, most of the fibers in the outer layer pointed toward random directions, confirming that the outer layer was comprised of random fibers. The uniaxially aligned fibers on the inner surface were able to promote axon extension owing to the contact guidance.[24a,26]

The NGC containing PCM particles was obtained by rolling up a tri-layer construct, which was fabricated by sandwiching PCM microparticles (pre-loaded with the factors) between the two layers of electrospun fibers.[27c] Figure S2 shows a schematic of the cross-sectional view of the NGC with a tri-layer structure for the wall, including uniaxially aligned fibers as the inner layer, random fibers as the outer layer, and a layer of electrosprayed PCM particles between them. Upon photothermal heating of the first, second, and distal third segment of the conduit with an 808-nm NIR laser at the designated time points, respectively, 6.2±1.4, 5.3±1.9, and 6.9±0.7 ng of NT-3 was released by diffusing out from the melted PCM. ChABC is sensitive to heat and can quickly lose its enzymatic activity at the body temperature. According to a previous study, the enzymatic activity of trehalose-stabilized ChABC could be maintained for up to 4 weeks at 37 °C *in vitro*.[29] Here, ChABC was stabilized by incubation with trehalose and the mixture was then encapsulated in the electrosprayed particles to preserve its enzymatic activity. Upon photothermal heating of the first, second, and distal third segment of the conduit with the NIR laser, the ChABC released from the conduit was able to digest more than 80% of decorin (*i.e.*, 83±7%, 86±6%, and 85±6%, respectively), confirming its preserved activity.

The NGCs containing collagen particles were also fabricated using the rolling-up method. Instead of in PCM particles, the factors were encapsulated in collagen particles using a co-axial electrospray method. Figure S3 shows the SEM image of the electrosprayed collagen particles loaded with factors, indicating the polydispersity in size. Figure 1A shows SEM image of the aligned fibers after coating with electrosprayed collagen particles. The particles adhered onto the surface of the fibers because of the residual solvent after electrospraying. Figure 1B shows the cumulative release profiles of NT-3 from the conduits containing the collagen particles, indicating continuous release over a 2-week period. It is difficult to measure the actual amount of the enzyme because of the presence of different types of proteins in the supernatant. We also evaluated the percentage of decorin digested by the ChABC released from the conduits. As shown in Figure 1C, the enzymatic activity could be preserved for one week and then dramatically decreased.

Because the microparticles, made of either PCM or collagen, were deposited as a thin layer between the two layers of electrospun fibers, it is difficult to resolve their morphology from the cross-sectional SEM images of the conduits. In general, the size of the conduit and the thickness of the wall were largely unaffected by the sandwiched microparticles. Meanwhile, the surface properties of both the inner and outer layers of the tri-layer conduit should be more or less identical to those of the plain conduit. Taken together, the difference in the release mechanism between the plain and factor-loaded groups was mainly determined by the material used for fabricating the microparticles. For the NGCs containing PCM microparticles, the factors were triggered to release due to the melting of the PCM upon the

irradiation with a laser. In contrast, for the NGCs containing collagen microparticles, the factors were released through diffusion, in a continuous and slow manner.

2.2 Continuous Release of NT-3 and ChABC Enhances Regeneration

Four treatments for nerve gap repair were initially evaluated in a rat model: autograft, plain NGC, NGC+hr-factors, and NGC+cr-factors (N=12 per group). Each animal was challenged with an 8-mm nerve gap. Twelve weeks after the injury was repaired, compound muscle action potentials (CMAPs) were evoked in the lateral gastrocnemius muscle, and the maximum amplitude and latency were measured.

CMAP amplitudes were the greatest in animals receiving autografts (Figure 2A), averaging about half of the amplitude found in the intact leg (35.4±0.6 mV, mean ± standard error of the mean, N=60). One-way ANOVA indicated significant differences between the groups [$F(3,44)=43.059$, $p=3.8\times10^{-13}$]. Autografts had significantly greater CMAP amplitudes than the other treatment groups (Tukey's post-hoc test, $p<10^{-5}$). The addition of continuously released factors to the NGCs significantly improved CMAP amplitudes relative to plain NGCs ($p<0.05$). However, timed, heat-release of the same factors appeared to inhibit recovery relative to the plain NGCs, although this did not quite reach statistical significance ($p=0.084$).

For CMAP latency, one-way ANOVA indicated significant differences between the groups [$F(3,23.264)=10.245$, $p=6.7\times10^{-6}$]. Similar to the CMAP amplitudes, CMAP latency was significantly shorter in animals receiving autografts than in animals receiving any of the other types of NGCs (Games-Howell post-hoc test, $p<0.05$, Figure 2B). No statistically significant difference was observed among the different types of NGCs.

2.3 Heating of the Conduit Does not Adversely Affect Regeneration

In order to better understand the reduced efficacy of the conduit containing heat-releasable factors, an additional cohort of animals receiving NGCs only containing the heat-labile PCM particles (NGC+matrix) was assessed (N=11). CMAP amplitudes in this cohort were nearly identical to the plain NGC group (Figure S4, 7.4±2.8 mV *vs.* 7.4±2.9 mV, respectively, Student's t test, $p=0.99$) and higher than the NGC+hr-factors group (7.4±2.8 mV *vs.* 4.7±2.9 mV, respectively, $p=0.037$). These results suggest that both heating the conduit and release of the melted PCM (lauric acid and stearic acid) from the conduit did not adversely impact nerve regeneration. Instead, the dose or pulsed nature of the release of the factors was likely the cause of the inferior response of the NGC+hr-factors group.

2.4 Histological Analysis of the Regenerated Nerves

Histological and immunofluorescence analyses were performed on the four treatment groups to evaluate the structure of the regenerated nerve within the graft or NGCs. We obtained 20-μm frozen sections from four to six animals per group, and sections near the midpoint of the graft or conduit were co-stained with antibodies against neurofilament 200 (NF200), labeling axons, and protein 0 (P0), labeling myelin. In all four groups, both myelinated and unmyelinated axons were apparent (Figure 3). There was no gross difference between the NGCs containing factors and those without. Sections were also co-stained for P0 and

laminin, an extracellular matrix marker. As expected, all four groups exhibited myelinated axons surrounded by the laminin-positive basal lamina with no obvious differences between groups (Figure 4).

We also obtained 0.7-μm thick sections from resin-embedded tissue treated with osmium tetroxide to stain myelin. Sections were counterstained with toluidine blue. Both myelinated axons and blood vessels were present within the graft and NGCs, as indicated by arrowheads and arrows in Figure 5, respectively. Between the axons and the interior surface of the conduit, there was a layer of tissue 50−200 μm thick that was generally devoid of axons. We hypothesized that this tissue may be a foreign body reaction directed against the NGC. Immunofluorescent staining was performed to detect NF200, prolyl 4-hydroxylase beta (P4HB, a marker for fibroblasts and macrophages producing collagen), CD68 (a phagocytic marker commonly found on macrophages) and smooth muscle actin (a fibroblast marker).[30] A band of $P4HB^+$ cells (Figure 6A) and a band of $CD68^+$ cells (Figure 6B) were observed between the axon-containing region and the plain NGC, suggesting the presence of an on-going foreign body reaction.[31] Fibroblasts were also identified in this region, but the abundance of these cells was highly variable from animal to animal. Semi-thin sections revealed cells that appeared to exhibit distended lysosomes or vacuoles (Figure 6C). This might represent the conduit material that had been phagocytosed.

The implications of the foreign body reaction for the efficacy of the NGC is unclear. The interior of the NGC is striated along its length to serve as a directional guide for axon growth. Direct contact between the axons and the conduit is not necessarily required, as this directionality can be transmitted through Schwann cells grown on the material.[32] However, it is unclear if the foreign body reaction can transmit this information in the same way or if it impedes the regrowth of axons, either by negatively affecting the direction of growth or limiting the space available for axons. Further study of this response is needed, but inhibition of the foreign body reaction may be a way to improve regeneration through the NGC.

2.5 Differences in Myelinated Axon Count Correlate with NGC Efficacy

In order to explain the negative effects of the NGC+hr-factors on motor recovery, we hypothesized that the pulsed release of the factors was inhibiting axonal growth into, through, or out of the NGCs. Myelinated axon counts at the midpoint of graft or NGCs and in the distal nerve were performed on semithin sections using stereology. For the mid-graft or mid-NGC samples, a Welch's ANOVA indicated a statistically significant difference between groups [$F(3,10.865)=11.648$, $p=1.0\times10^{-3}$]. Autografts had a significantly greater number of myelinated axons than any of the conduit groups (Games-Howell post-hoc test, $p<0.04$, Figure 7A), and NGC+cr-factors had a significantly greater number of axons than plain NGC and NGC+hr-factors ($p<0.03$). There was no statistical difference between plain NGC and NGC+hr-factors ($p=0.64$). Similar to the mid-conduit data, one-way ANOVA analysis of the distal nerve indicated a statistically significant difference between groups [$F(3,19)=33.407$, $p=8.8\times10^{-8}$]. Animals with autografts had significantly greater axon counts than those with any type of conduit (Tukey's post-hoc test, $p<10^{-4}$; Figure 7B), and axon counts in NGC+cr-factors were significantly greater than those in NGC+hr-factors

(p<0.005). No significant difference was detected between the NGC+cr-factors and plain NGC groups (p=0.40).

Notably, the axon counts in the distal nerve were generally higher than the axon counts within the conduits. A paired t-test was performed to compare the axon counts distal to and within the conduits for each type of conduit. The distal axon count was statistically higher for NGC+hr-factors (p=0.04) and for NGC+cr-factors (p=1.6×10^{-4}). The average fold change in axon counts between mid-NGCs and the distal nerve for plain NGC, NGC+hr-factors, and NGC+cr-factors was 1.7±0.6, 1.9±0.3, 1.5±0.3, respectively (average ± standard deviation). In contrast, for animals receiving an autograft, the fold change was lower (1.2±0.4). These results suggest that axons were underwent sprouting between the middle of the conduit and the distal nerve, possibly at the interface between the two.[33]

Following nerve transection and repair, regenerating axons can produce multiple collateral sprouts. These sprouts can grow along anterograde and retrograde directions,[34] resulting in an increase in axon number both proximal and distal to the repair site on the order of 1.5- to 5-fold.[35] Presumably, the axons are responding to a non-soluble cue, possibly coming from the laminin or Schwann cells.[36] In addition, collateral sprouts from a single neuron can project to different branches of the nerve and perhaps innervate multiple targets.[37]

The implications of collateral sprouting and pruning for motor function in the current study is unclear. When axons sprout collaterals, these projections can end up traversing different nerve branches,[38] potentially allowing a single motor neuron to innervate two or more opposing muscle groups.[33,39] If this occurs frequently enough, it would negatively affect motor function by preventing useful control of these muscles. Additional studies focusing on behavioral tasks will be needed to address this question.

3. Conclusion

We have studied the efficacy of NGCs fabricated from electrospun fibers and integrated with factors for the repair of peripheral nerve injury in a rat model. The combination of NT-3 and ChABC is capable of enhancing the repair of the nerve gap when applied to NGCs. However, the method of release significantly impacts whether the effect is positive or negative. The pulsed release of NT-3 and ChABC inhibits reinnervation of the muscle through an unknown mechanism, resulting in fewer myelinated axons entering the distal nerve stump. In contrast, continuous release of the factors significantly improves the efficacy of the NGCs, increasing the maximal CMAP amplitude by 42% and the number of axons in the midpoint. Despite this improvement, the NGC+cr-factors system is still inferior to the autograft. Future studies will be needed to determine if combining other agents, such as Schwann cells, with slow-release factors can further increase the effectiveness of these conduits and make them comparable to an autograft.

4. Experimental Section

Fabrication of nerve guidance conduits.

We fabricated three types of NGCs: plain conduit, conduit containing PCM particles for the heat-controlled release, and conduit containing collagen particles for continuous release. The inner diameter of the conduits was about 1.5 mm. The plain conduit was obtained by rolling up a bilayer of electrospun fiber mats. Briefly, a PCL (M_n: 80kDa) solution at a concentration of 12 wt.% was prepared by dissolving polycaprolactone pellets in a mixture of dichloromethane and *N*, *N*-dimethylformamide (6:4, v/v). Then, a bilayer mat consisting of uniaxially aligned and random fibers for the bottom and top layers, respectively, was fabricated by electrospinning with a rotating mandrel and a piece of aluminum foil as the collector. The bottom layer was treated by O_2 plasma for 2 min, and then both sides of the mat were sterilized with UV for 30 min. Afterwards, a conduit was obtained by rolling up the bilayer mat, with the layer composed of uniaxially aligned fibers as the inner wall, and sealing the edges with the same polymer solution for electrospinning. The plain conduit was characterized using SEM. The conduit was frozen-embedded in Tissue-Tek® optimum cutting temperature (O.C.T.) compound (VWR, Radnor, PA) and then sectioned using cryostat (CryoStar NX70), along the direction perpendicular to the long axis, to obtain samples with a thickness of 80 μm. Afterwards, the samples were washed with water and dried at room temperature prior to SEM analysis.

The NGC for the heat-release of factors (NGC+hr-factors) was obtained by rolling up a tri-layer construct which was fabricated through an integration of the electrospinning process with electrospray, as previously described.[27c] After the electrospinning of uniaxially aligned fibers, PCM particles containing the factors were electrosprayed onto the surface of the fibers using a co-axial electrospray method. The PCM (a mixture of lauric acid and stearic acid at a mass ratio of 8:2) dissolved in a mixture of ethanol and dichloromethane (20:80 by vol.) at a concentration of 20% was used as the outer fluid. The solution containing NT-3/heparin and indocyanine green dissolved in a 0.5 wt.% aqueous gelatin solution at concentrations of 100 μg/mL and 1 mg/mL, respectively, was used as the inner fluid. After electrospray for 2.5 min, the inner fluid was replaced with a solution of the mixture of ChABC (10 U/0.5 mL), trehalose (1 M) and indocyanine green (1 mg/mL), and another 2.5 min of electrospray was applied. The feeding speeds of the outer and inner fluids were set to 3.0 and 1.0 mL/h, respectively. Afterwards, a layer of random fibers was deposited on top. The NGCs containing indocyanine green-loaded PCM particles were also fabricated as a control group.

The NGC for the continuous release of factors (NGC+cr-factors) was fabricated by integrating factors-encapsulated collagen particles between the two layers of electrospun fibers. A solution of collagen at a concentration of 5 w/v% was prepared in 70 v/v% aqueous acetic acid and used as the outer fluid during the electrospray process, while the solution containing NT-3 or ChABC/trehalose was used as the inner fluid. The flow rates for the outer and inner fluids were set to 1.5 and 0.5 mL/h, respectively. Followed by the electrospray of particles containing NT-3 on the aligned fibers for 5 min, the particles containing ChABC were electrosprayed for another 5 min, and then random fibers were

deposited on top. The morphologies of the collagen particles and aligned fibers deposited with collagen particles were characterized using a scanning electron microscope.

Release of factors from NGCs.

The factors in NGCs containing PCM particles were trigged to be released upon photothermal heating. The NGC was placed in a well of a 24-well plate, and 500 μL of deionized water was added to the well. The first third of the conduit was then exposed to an 808-nm diode laser at a power density of 1.0 W/cm^2. The temperature of the conduit was monitored using an infrared camera to assure the conduit was not heated to over 42 °C. The conduit was rotated to assure the whole surface of the first third of the conduit was exposed to the laser. After 1 day of irradiation, the supernatant was retrieved from each sample and fresh medium was added. After 2 and 4 days, the irradiation procedure was repeated, respectively, to trigger the release of factors from the second and the distal third of the conduit. The content of NT-3 in the supernatant was measured using NT-3 ELISA following the manufacture's protocol. The enzymatic activity of ChABC released from the conduit was measured using the dimethylmethylene blue assay as previously described.[29,40] Briefly, the collected supernatant was reacted with 10 μL of decorin (5 μg) at 37 °C for 2 h. Then, the dimethylmethylene blue reagent was added and the absorbance at 530 nm was recorded.

For the NGCs containing collagen particles, the release of the factors was evaluated under static conditions. Briefly, the conduit was immersed in 500 μL of phosphate buffer solution and incubated at 37 °C. At each time point, the supernatant was collected and replaced with fresh solution. The amount of NT-3 in the supernatant was then measured using the ELISA assay. The collected supernatant was also mixed with decorin, incubated at 37 °C, and then analyzed with the dimethylmethylene blue assay.

Nerve gap repair.

All animal experiments were approved by the Emory University Institutional Animal Care and Use Committee. For these studies an acute sciatic nerve injury was modeled in Lewis rats (250−300g in weight at the time of surgery). This model was chosen because they exhibit fewer complications following nerve injury. For each group, 12 rats were used to evaluate the nerve gap repair. Rats were randomly assigned to treatment groups using the following strategy. Prior to study initiation, each animal was assigned an ID. In addition, each animal ID was paired with a random number generated within an Excel spreadsheet. The animals were then sorted lowest to highest based on the randomly generated number. The lowest numbers were assigned to the autograft group, the second lowest number to the plain NGC group, *etc.*

At approximately 70 days of age, the animals underwent a sciatic nerve injury and repair. The animals were anesthetized with 2% isoflurane and placed in the prone position. The left hind leg was elevated with a 15-mL conical tube. Fur was removed from the surgical field using electric clippers, and the skin was sterilized with three repeated applications of betadine and isopropanol. A sterile drape was then applied around the planned incision site. An incision was made through the skin roughly parallel to the femur, and the anterior and posterior muscles were separated by bluntly dissecting through the lateral intermuscular

septum to expose the sciatic nerve. The nerve was freed from the surrounding tissue using fine forceps and micro scissors.

To create a nerve gap injury, an 8-mm section of the sciatic nerve was excised proximal to the branching of the tibial and common peroneal nerves. Due to the variability in the branching of the sural nerve in this region, this nerve was sacrificed in all animals to obtain a consistent challenge. For animals in the autograft group, the excised nerve segment was flipped and reattached using end-to-end anastomosis with four 10–0 sutures per joint. For animals receiving conduits, a 10-mm long conduit was used to span the gap. The proximal and distal nerve stumps were inserted 1 mm into either side of the conduit and secured with 10–0 suture, creating an 8-mm challenge. After the nerve repair, the muscle was closed with 4–0 vicryl suture and the skin was closed with 4–0 suture. For animals receiving infrared laser irradiation, the locations on the skin directly above the ends of the conduit were marked with a tattoo. The animal was then placed in a warm cage to recover. External sutures were removed one week after surgery.

Near-infrared irradiation.

For animals implanted with conduits containing heat releasable factors, the conduit was heated through the skin and muscle using a NIR laser (LDCU12/9047, Power Technology Inc., Little Rock, Arizona) one week, two weeks, and three weeks following surgery. For each time point, the laser head was positioned 4 mm from the skin and centered above the first, second, or distal third of the conduit, respectively. The laser was applied for 10 min to raise the temperature of the conduit to 40−42 °C. This approach was designed to release the factors just ahead of the leading edge of the axons at each time point.

Compound muscle action potential measurements.

CMAPs were measured using a Nicolet Endeavor CR System (Natus Neurology, Inc., Middleton, WI) using 500 Hz and 3,000 Hz for the low and high band-pass filters, respectively, and with the gain set to 100x. Twelve weeks after nerve repair, the animals were anesthetized, and the left and right sciatic nerves were exposed as described above. A piece of Parafilm (Bemis Company, Neenah, WI) was placed under the nerve to create a non-conductive barrier. An incision was also made in the skin covering the lateral gastrocnemius muscle to allow placement of a recording electrode (74612–100/1/20, Ambu, Columbia, MD) in this muscle. A second incision was made in the skin above the lumbar spine to place a ground electrode. A reference electrode was placed under the skin on the side of the foot. A bipolar electrode was used to gently lift the nerve proximal to the graft or conduit. A series of electric stimuli were delivered with increasing amperage while recording from the lateral gastrocnemius until the amplitude of the CMAP became maximal. The latency, maximum amplitude, minimum amplitude, and duration of the CMAP were measured and recorded. Data are reported as the mean ± standard error of the mean.

Histology and immunofluorescence.

After CMAPs data were recorded, the sciatic nerves were harvested, and the animals were euthanized. The nerves/NGCs of four to six animals per group were immediately frozen in

Tissue-Tek® O.C.T. Compound for immunofluorescence analysis. The remainder were fixed in 4% glutaraldehyde and processed for thin sections to count myelinated axons.

For immunofluorescence staining, 20 μm thick sections were obtained on a Leica CM1950 cryostat (Wetzlar, Germany). Sections were blocked in 5% normal goat serum (#005–000-121, Jackson ImmunoResearch, West Grove, PA) for 30 min prior to staining. The following antibodies and dilutions were used: rabbit anti-NF200 (1:1000, ab8135, Abcam, Cambridge, MA), chicken anti-P0 (1:100, ab39375, Abcam), rabbit anti-laminin (1:1000, ab30320, Abcam), mouse anti-P4HB (1:250, ab2792, Abcam), rabbit anti-CD68 (1:500, ab125212, Abcam), rabbit anti-smooth muscle actin (1:100, ab5694, Abcam)), mouse anti-NF200 (1:1000, ab7795, Abcam), FITC-conjugated goat anti-rabbit (1:250, 111–095-144, Jackson ImmunoResearch), TRITC-conjugated goat anti-mouse (1:250, 115–025-166, Jackson ImmunoResearch), and TRITC-conjugated goat anti-chicken (1:250, 103–025-155, Jackson ImmunoResearch). Images were obtained on a Nikon Eclipse E400 microscope (Tokyo, Japan) with a Nikon Digital Sight controller and DS-Fi1 camera. For each channel, the images were collected in gray scale, pseudocolored, and overlaid using NIS-Elements (Nikon).

For axon counts, the nerves samples were fixed with 2.5% glutaraldehyde in 0.1 M cacodylate buffer (pH 7.4). Samples were then rinsed with 0.1 M cacodylate buffer (pH 7.4) twice before post-fixation in 1% osmium tetroxide for 1 h. After additional buffer rinses, samples were dehydrated through an ethanol series to 100% ethanol. Samples were infiltrated with a mixture of propylene oxide and Eponate 12 resin (Ted Pella Inc., Redding, CA) and then pure Eponate 12 resin overnight. Samples were embedded in Beem capsules and then placed in a 60 °C oven for polymerization. Semi-thin sections were cut with a Leica UltraCut microtome at 0.7 μm and then placed on glass slides. Sections were stained with Toluidine Blue before placing coverslips on slides. Axons were counted using a Stereologer system (SRC Biosciences, Tampa, FL) featuring Stereologer 3.0 CP version 2 software, a Leica DM2500 microscope, HDXS 3CCD-1080P camera (Optronics) and Pro-lite 1080p 2MP controller box. Two individuals blinded to the treatment group independently counted the number of axons in each sample. Their results were averaged to produce an axon count for each sample.

Statistics.

All statistical tests were carried out using IBM SPSS Statistics version 24 on an Apple iMac with a 4 GHz Intel Core i7 processor and 16 GB of DDR3 RAM running OS 10.11.6. For comparisons of CMAP amplitudes and distal axon counts among the four treatment groups, a one-way ANOVA with a Tukey post-hoc test was used to determine significant differences between groups. For CMAP latencies and mid-NGC axon counts, analysis revealed a violation of the homogeneity of variances, so a Welch's ANOVA with a Games-Howell post-hoc test was used instead. For the comparisons involving the NGC+matrix group, a two-tailed t test was used. Significance was set at $p \leq 0.05$ for all statistical analyses. Data are reported as the mean ± standard error of the mean except for the fold change in axon counts between the conduit and distal nerve, which are reported as the mean ± standard deviation.

Supplementary Material

Refer to Web version on PubMed Central for supplementary material.

Acknowledgements

This work was supported by a grant from the National Institutes of Health (R01 EB020050) and startup funds from the Georgia Institute of Technology. This study was also supported by the Robert P. Apkarian Integrated Electron Microscopy Core (RPAIEMC), which is subsidized by the Emory University School of Medicine and the Emory College of Arts and Sciences and is one of the Emory Integrated Core Facilities. Many thanks to Art English for helpful discussions regarding this project.

References

[1]. a) Daly W, Yao L, Zeugolis D, Windebank A, Pandit A, J. R. Soc. Interface 2012, 9, 202; [PubMed: 22090283] b) Campbell WW, Clin. Neurophysiol 2008, 119, 1951; [PubMed: 18482862] c) Taylor CA, Braza D, Rice JB, Dillingham T, Am. J. Phys. Med. Rehabil 2008, 87, 381. [PubMed: 18334923]

[2]. Schmidt CE, Leach JB, Annu. Rev. Biomed. Eng 2003, 5, 293. [PubMed: 14527315]

[3]. Hoke A, Nat. Clin. Pract. Neurol 2006, 2, 448. [PubMed: 16932603]

[4]. Noble J, Munro CA, Prasad VS, Midha R, J. Trauma 1998, 45, 116. [PubMed: 9680023]

[5]. a) Lee SK, Wolfe SW, J. Am. Acad. Orthop. Surg 2000, 8, 243; [PubMed: 10951113] b) Ichihara S, Inada Y, Nakamura T, Injury. 2008, 39 Suppl 4, 29. [PubMed: 18804584]

[6]. Isaacs J, Browne T, Hand (NY) 2014, 9, 131.

[7]. Kehoe S, Zhang XF, Boyd D, Injury 2012, 43, 553. [PubMed: 21269624]

[8]. a) Quigley AF, Bulluss KJ, Kyratzis IL, Gilmore K, Mysore T, Schirmer KS, Kennedy EL, O'Shea M, Truong YB, Edwards SL, Peeters G, Herwig P, Razal JM, Campbell TE, Lowes KN, Higgins MJ, Moulton SE, Murphy MA, Cook MJ, Clark GM, Wallace GG, Kapsa RM, J. Neural. Eng 2013, 10, 016008;b) <Sterne GD, Brown RA, Green CJ, Terenghi G, Eur. J. Neurosci 1997, 9, 1388; [PubMed: 9240396] c) Zong H, Zhao H, Zhao Y, Jia J, Yang L, Ma C, Zhang Y, Dong Y, Neural. Regen. Res 2013, 8, 1262. [PubMed: 25206420]

[9]. a) Wood MD, Moore AM, Hunter DA, Tuffaha S, Borschel GH, Mackinnon SE, Sakiyama-Elbert SE, Acta. Biomater 2009, 5, 959; [PubMed: 19103514] b) Barras FM, Pasche P, Bouche N, Aebischer P, Zurn AD, J. Neurosci. Res 2002, 70, 746. [PubMed: 12444596]

[10]. Cao J, Sun C, Zhao H, Xiao Z, Chen B, Gao J, Zheng T, Wu W, Wu S, Wang J, Dai J, Biomaterials 2011, 32, 3939. [PubMed: 21397941]

[11]. a) Xia B, Lv Y, Mater. Sci. Eng. C Mater. Biol. Appl 2018, 82, 253; [PubMed: 29025656] b) Nikolaev SI, Gallyamov AR, Mamin GV, Chelyshev YA, Bull. Exp. Biol. Med 2014, 157, 155. [PubMed: 24915952]

[12]. Wong V, Arriaga R, Ip NY, Lindsay RM, Eur. J. Neurosci 1993, 5, 466. [PubMed: 7505167]

[13]. Griesbeck O, Parsadanian AS, Sendtner M, Thoenen H, J. Neurosci. Res 1995, 42, 21. [PubMed: 8531223]

[14]. Munson JB, Shelton DL, McMahon SB, J. Neurosci 1997, 17, 470. [PubMed: 8987771]

[15]. Yamauchi J, Chan JR, Shooter EM, Proc. Natl. Acad. Sci. U.S.A 2003, 100, 14421.

[16]. a) Meier C, Parmantier E, Brennan A, Mirsky R, Jessen KR, J. Neurosci 1999, 19, 3847; [PubMed: 10234017] b) Sahenk Z, Oblinger J, Edwards C, Exp. Neurol 2008, 212, 552. [PubMed: 18511043]

[17]. Sterne GD, Coulton GR, Brown RA, Green CJ, Terenghi G, J. Cell Biol 1997, 139, 709. [PubMed: 9348287]

[18]. a) Yurchenco PD, Patton BL, Curr. Pharm. Des 2009, 15, 1277; [PubMed: 19355968] b) Graham JB, Muir D, PLoS One 2016, 11, e0167682.

[19]. a) Zuo J, Hernandez YJ, Muir D, J. Neurobiol 1998, 34, 41; [PubMed: 9469617] b) Braunewell KH, Pesheva P, McCarthy JB, Furcht LT, Schmitz B, Schachner M, Eur. J. Neurosci 1995, 7, 805;

[PubMed: 7620627] c) Snow DM, Lemmon V, Carrino DA, Caplan AI, Silver J, Exp. Neurol 1990, 109, 111. [PubMed: 2141574]

[20]. a) Lane JM, Bora FW Jr., Pleasure D, J. Bone Joint Surg. Am 1978, 60, 197; [PubMed: 641084] b) Ngeow WC, Oral Surg Oral Med Oral Pathol Oral Radiol Endod 2010, 109, 357. [PubMed: 20219599]

[21]. Atkins S, Smith KG, Loescher AR, Boissonade FM, O'Kane S, Ferguson MWJ, Robinson PP, Neuroreport. 2006, 17, 1245. [PubMed: 16951563]

[22]. Groothuis J, Ramsey NF, Ramakers GM, van der Plasse G, Brain Stimul. 2014, 7, 1. [PubMed: 23941984]

[23]. Krekoski CA, Neubauer D, Zuo J, Muir D, J. Neurosci 2001, 21, 6206. [PubMed: 11487643]

[24]. a) Wu T, Mo X, Xia Y, Adv. Healthc. Mater, 2020, 9, 1901761;b) Xie J, MacEwan MR, Liu W, Jesuraj N, Li X, Hunter D, Xia Y, ACS Appl. Mater. Interfaces 2014, 6, 9472; [PubMed: 24806389] c) Wu T, Li D, Wang Y, Sun B, Li D, Morsi Y, El-Hamshary H, Al-Deyab SS, Mo X, J. Mater. Chem. B 2017, 5, 3186; [PubMed: 32263716] d) Wang J, Zheng W, Chen L, Zhu T, Shen W, Fan C, Wang H, Mo X, ACS Biomater. Sci. Eng 2019, 5, 2444;e) Xue C, Zhu H, Tan D, Ren H, Gu X, Zhao Y, Zhang P, Sun Z, Yang Y, Gu J, Gu Y, Gu X, J. Tissue Eng. Regen. Med 2018, 12, e1143.

[25]. Woodruff MA, Hutmacher DW, Prog. Polym. Sci 2010, 35, 1217.

[26]. a) Corey JM, Lin DY, Mycek KB, Chen Q, Samuel S, Feldman EL, Martin DC, J. Biomed. Mater. Res. A 2007, 83A, 636;b) Xie J, Liu W, MacEwan MR, Bridgman PC, Xia Y, ACS Nano 2014, 8, 1878–1885. [PubMed: 24444076]

[27]. a) Hyun DC, Levinson NS, Jeong U, Xia Y, Angew. Chem. Int. Edit 2014, 53, 3780;b) Choi SW, Zhang Y, Xia Y, Angew Chem. Int. Ed 2010, 49, 7904;c) Xue J, Zhu C, Li J, Li H, Xia Y, Adv. Funct. Mater 2018, 28, 1705563;d) Qiu J, Huo D, Xue J, Zhu G, Liu H, Xia Y, Angew Chem. Int. Ed 2019, 58, 10606.

[28]. Jayaraman P, Gandhimathi C, Venugopal JR, Becker DL, Ramakrishna S, Srinivasan DK, Adv. Drug Deliv. Rev 2015, 94, 77. [PubMed: 26415888]

[29]. Lee H, McKeon RJ, Bellamkonda RV, Proc. Natl. Acad. Sci. U. S. A 2010, 107, 3340. [PubMed: 19884507]

[30]. Pilling D, Fan T, Huang D, Kaul B, Gomer RH, PLoS One 2009, 4, e7475.

[31]. Dondossola E, Holzapfel BM, Alexander S, Filippini S, Hutmacher DW, Friedl P, Nat. Biomed. Eng 2016, 1, 0007.

[32]. Xue J, Yang J, O'Connor DM, Zhu C, Huo D, Boulis NM, Xia Y, ACS Appl. Mater. Interfaces 2017, 9, 12299.

[33]. Watrous WG, Proc. Soc. Exp. Biol. Med 1940, 44, 541.

[34]. Mackinnon SE, Dellon AL, O'Brien JP, Muscle Nerve 1991, 14, 1116. [PubMed: 1745287]

[35]. a) Shawe GD, Br. J. Surg 1955, 42, 474; [PubMed: 14363682] b) Evans DH, Murray JG, Anat. Rec 1956, 126, 311; [PubMed: 13394944] c) Jenq CB, Coggeshall RE, Brain Res 1984, 310, 107. [PubMed: 6478232]

[36]. a) Masuda-Nakagawa LM, Muller KJ, Nicholls JG, Proc. Natl. Acad. Sci. U. S. A 1993, 90, 4966; [PubMed: 8506343] b) Armstrong SJ, Wiberg M, Terenghi G, Kingham PJ, Tissue Eng. 2007, 13, 2863. [PubMed: 17727337]

[37]. Brushart TM, J. Neurosci 1993, 13, 2730. [PubMed: 8501535]

[38]. a) Brushart TM, Jari R, Verge V, Rohde C, Gordon T, Exp. Neurol 2005, 194, 221; [PubMed: 15899259] b) Robinson GA, Madison RD, Restor. Neurol. Neurosci 2013, 31, 451. [PubMed: 23648674]

[39]. a) Langley JN, Anderson HK, J. Physiol 1904, 31, 365; [PubMed: 16992733] b) Esslen E, Electroencephalogr Clin. Neurophysiol 1960, 12, 738. [PubMed: 13820840]

[40]. Liu T, Xu J, Chan BP, Chew SY, J. Biomed. Mater. Res. A 2012, 100, 236. [PubMed: 22042649]

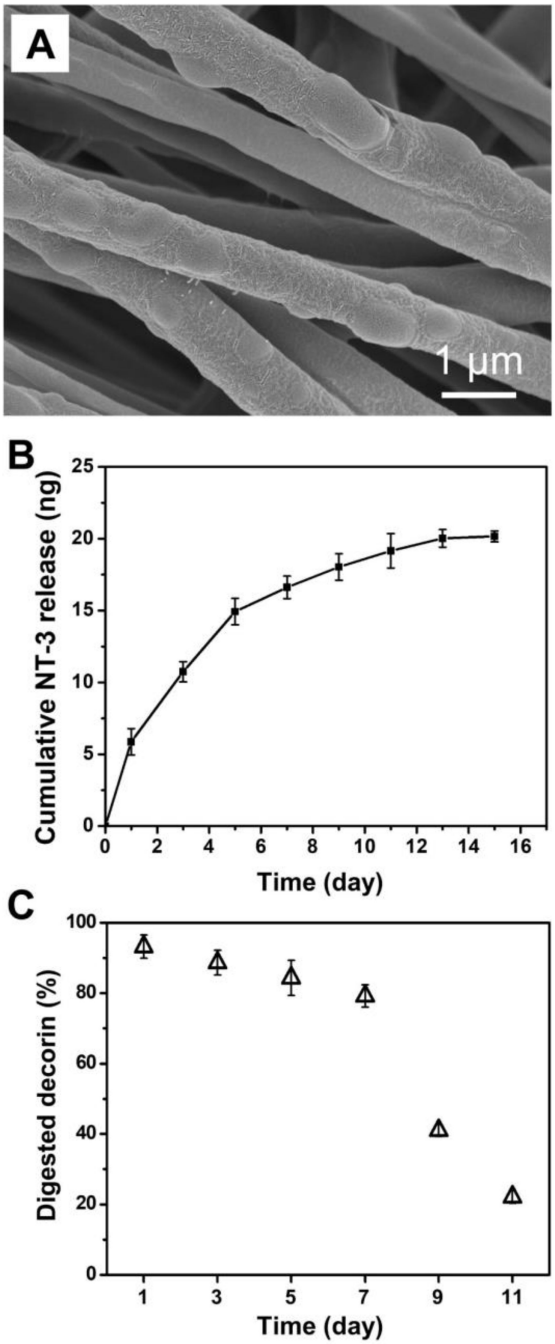

Figure 1.

(A) SEM image of the collagen particles deposited on the surface of uniaxially aligned fibers. (B) The cumulative release profile of NT-3 from the conduits loaded with factor-containing collagen particles. (C) Percentage of decorin digested by ChABC released from the conduits loaded with factor-containing collagen particles. The error bars represent one standard deviation.

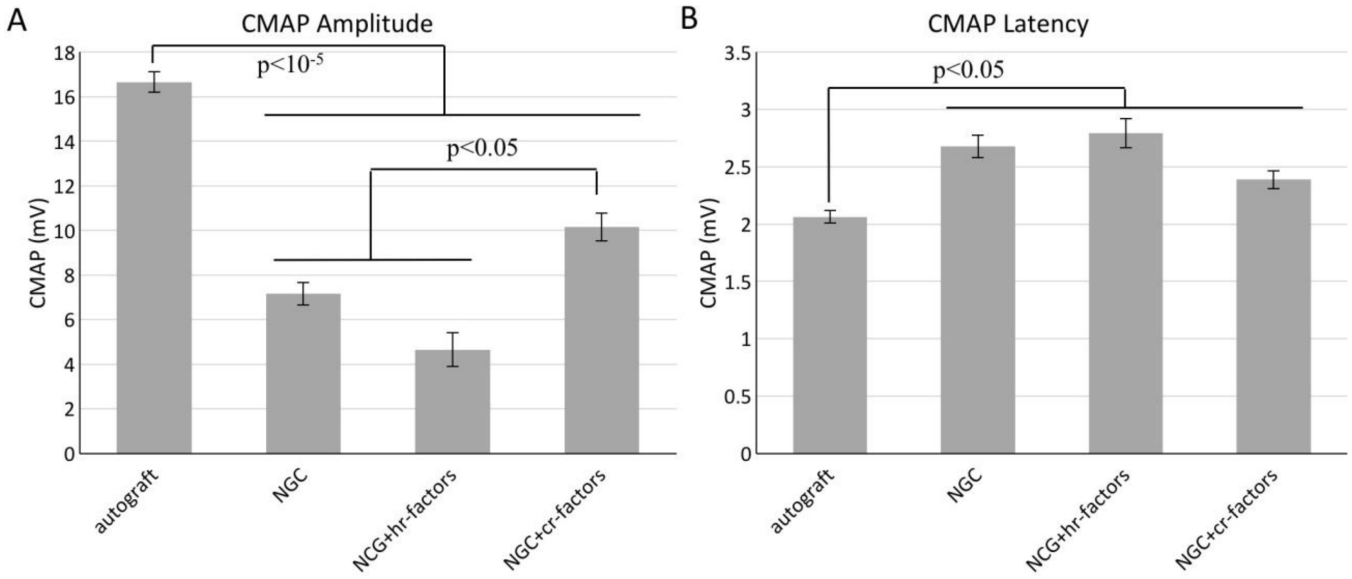

Figure 2.

The maximal CMAP amplitude and CMAP latency recorded for each animal (N=12 per group), with the data being presented as mean ± standard error of the mean. (A) Autograft resulted in significantly higher CMAP amplitudes relative to all of the NGC groups. Animals receiving NGC+cr-factors had significantly higher amplitudes than those receiving plain NGC or NGC+hr-factors. (B) CMAP latency was significantly shorter in the autograft group than in any of the conduit groups ($p<0.05$).

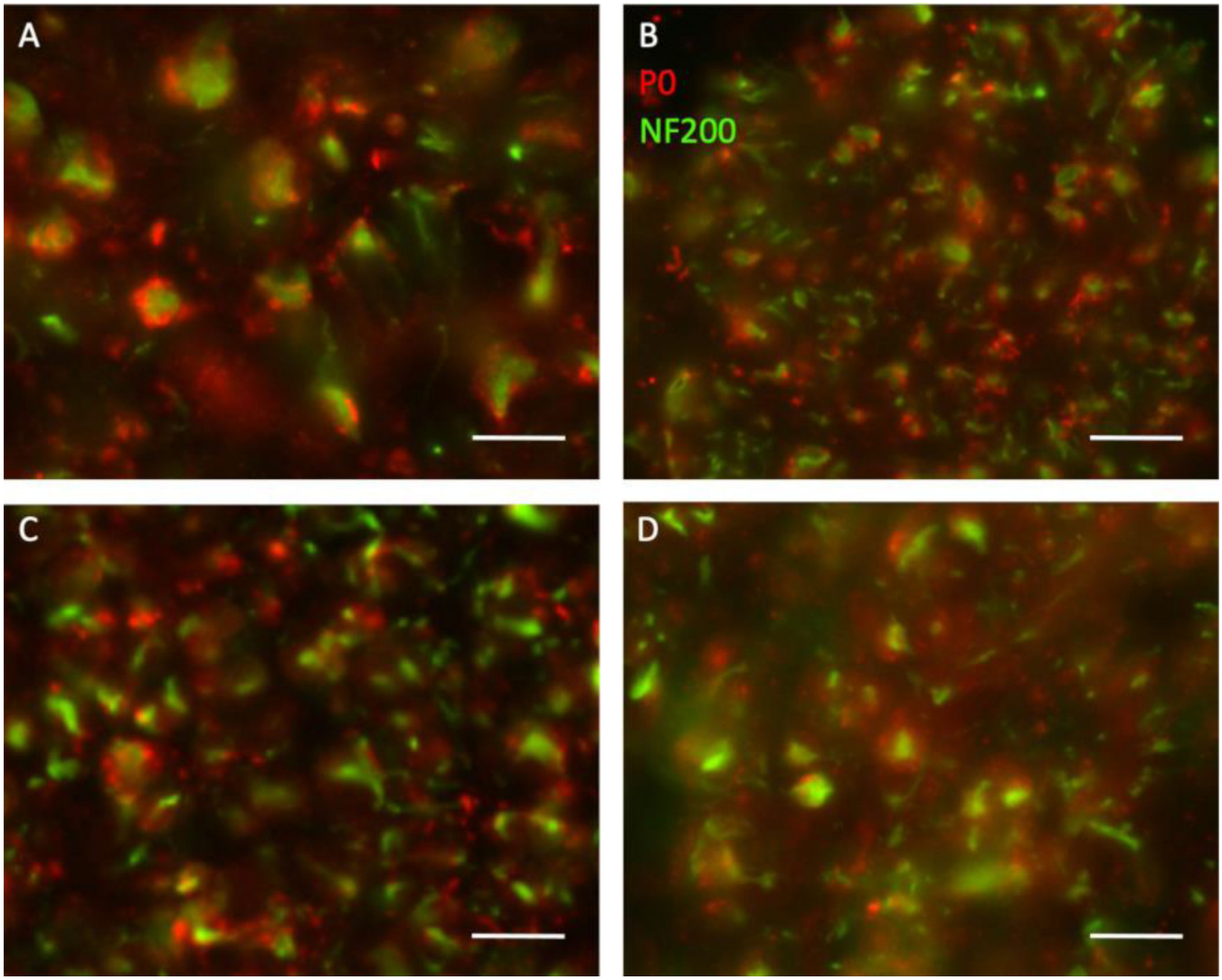

Figure 3.

Immunofluorescent staining for myelin and neurofilament. With 4−6 animals per group, 20-μm frozen sections were obtained and stained with antibodies against myelin protein 0 (P0, red) and neurofilament 200 (NF200, green). The fluorescence micrographs show representative sections from the midpoint of the (A) autograft, (B) plain NGC, (C) NGC+hr-factors, and (D) NGC+cr-factors. $NF200^{+}$ axons surrounded by $P0^{+}$ myelin were found throughout the grafts and NGCs. No gross differences were observed between the groups. The scale bars represent 11.25 μm.

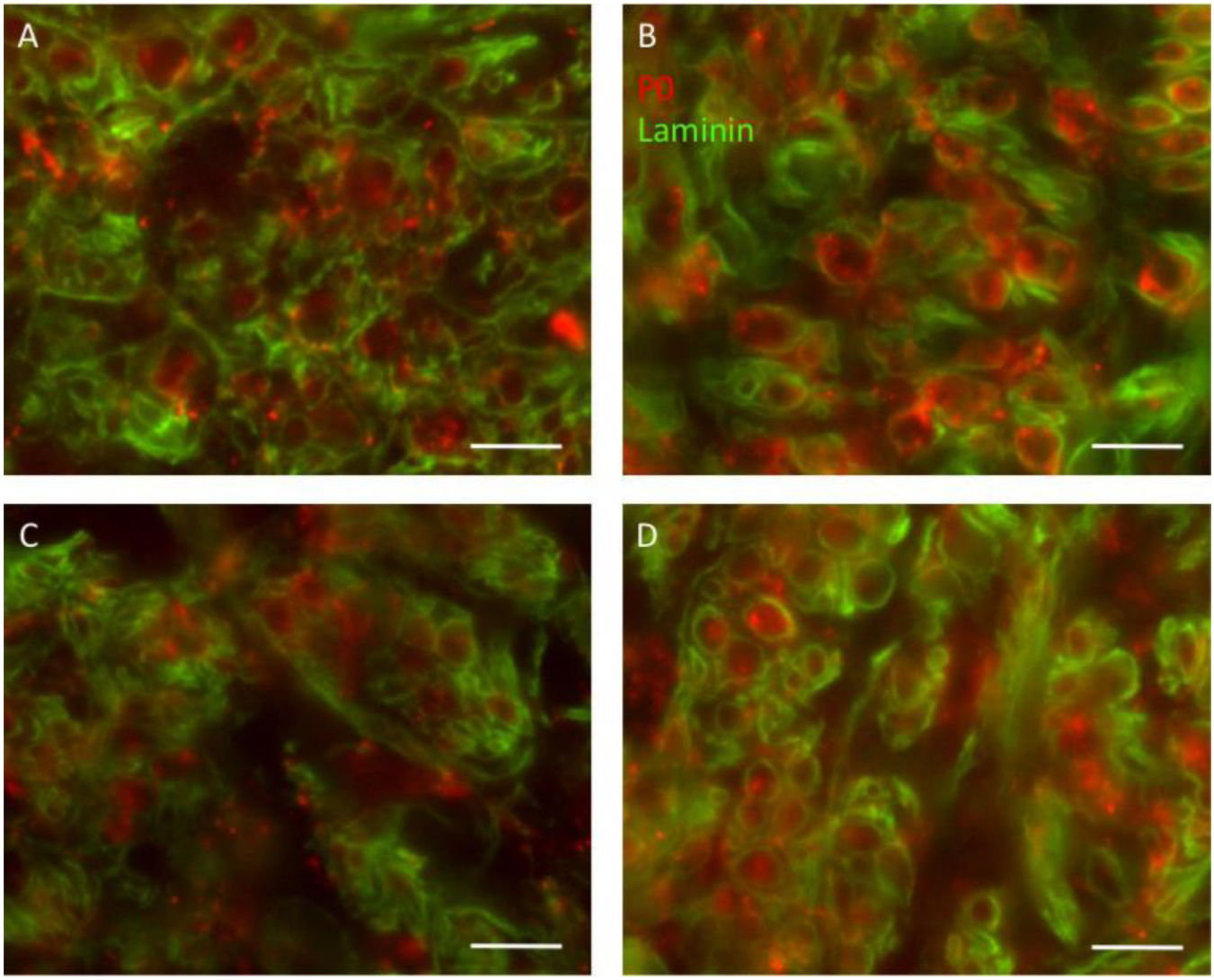

Figure 4.

Immunofluorescent staining for myelin and laminin. With 4−6 animals per group, 20-μm frozen sections were obtained and stained with antibodies against myelin protein 0 (P0, red) and laminin (green). The fluorescence micrographs show representative sections from the midpoint of the (A) autograft, (B) plain NGC, (C) NGC+hr-factors, and (D) NGC+cr-factors. Myelinated axons were surrounded by a ring of laminin that formed the basement membrane. No gross differences were observed between the groups. The scale bars represent 11.25 μm.

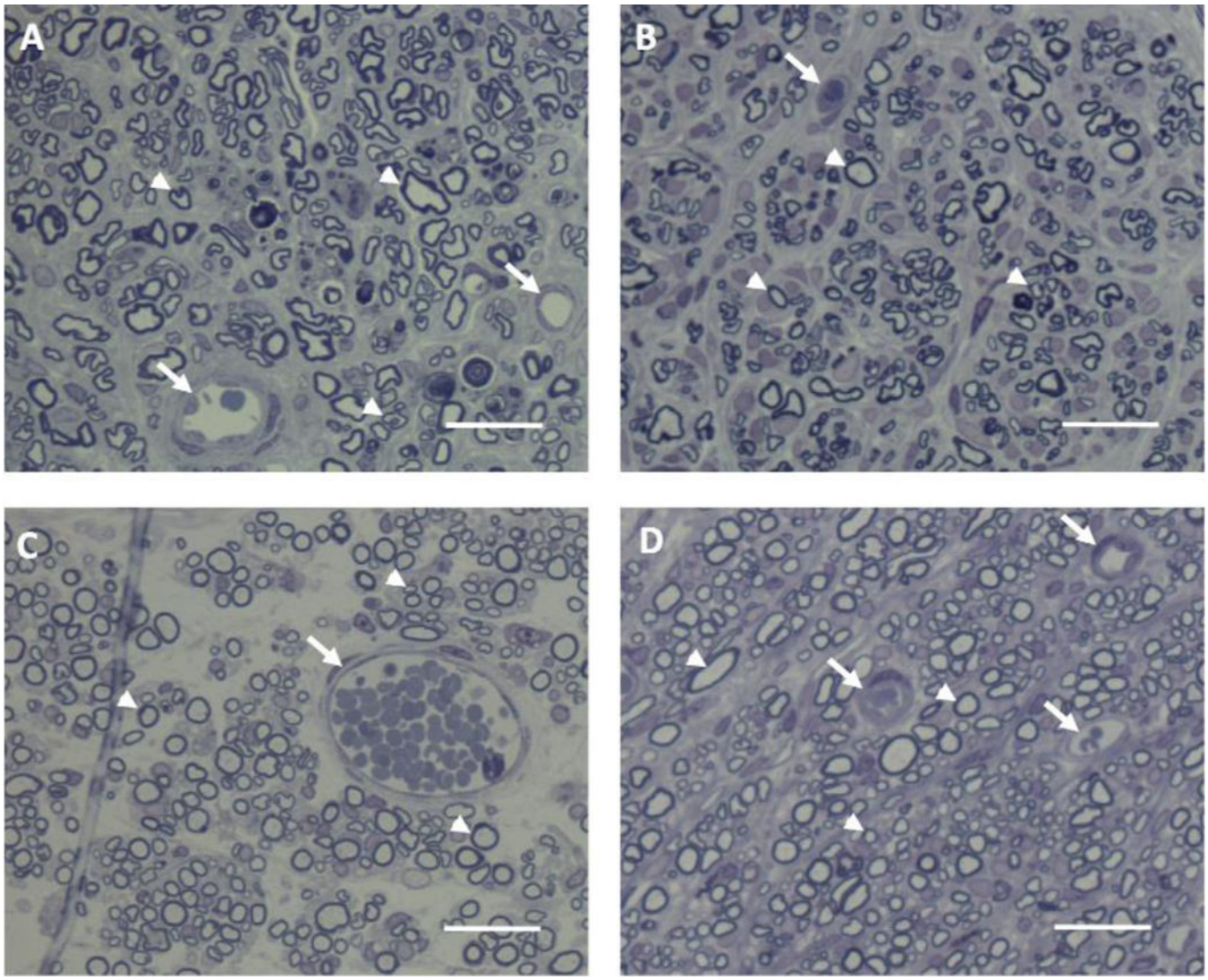

Figure 5.

Histochemical analysis of the semi-thin sections. With 4−6 animals per group, the tissue was stained with osmium tetroxide. Sections of 0.7 μm in thickness were obtained and counterstained with toluidine blue. The micrographs show representative sections from the midpoint of the (A) autograft, (B) plain NGC, (C) NGC+hr-factors, and (D) NGC+cr-factors. All animals exhibited myelinated axons (arrowheads) and blood vessels (arrows). The line across the NGC tissue in (C) is an artifact from tissue processing. The scale bars represent 25 μm.

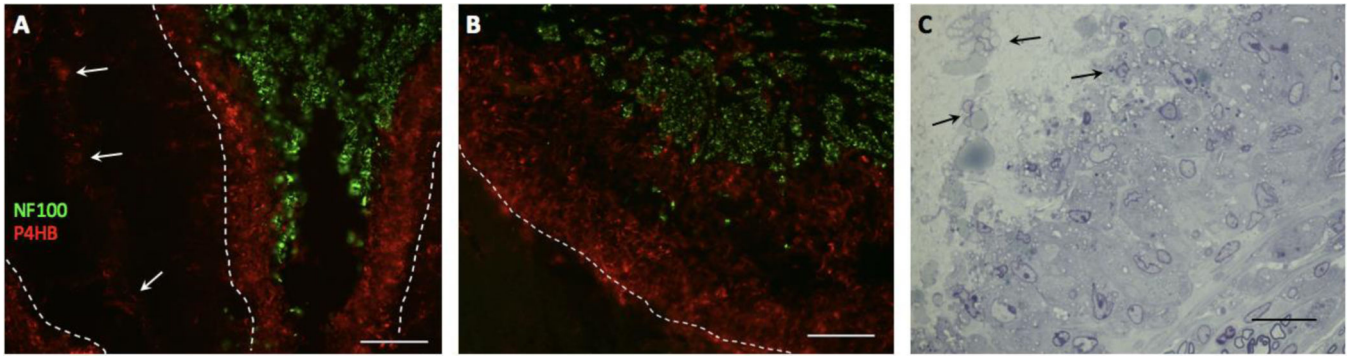

Figure 6.

(A) With 4−6 animals per group, 20-μm frozen sections were obtained and stained for prolyl 4-hydroxylase β (P4HB, red) and neurofilament 200 (NF200, green). The fluorescence micrograph shows a representative section from an animal receiving a plain NGC. The conduit is indicated by a dashed, white line. Between the $NF200^+$ axons and the conduit is a layer of $P4HB^+$ cells, presumably caused by a foreign body reaction. Some cells have migrated into the conduit (arrows). (B) Similarly, this region contains $CD68^+$ macrophages (red), again suggesting a foreign body reaction. (C) With 6−8 animals per group, the tissue was stained with osmium tetroxide. Sections of 0.7 μm in thickness were obtained and counterstained with toluidine blue. The micrograph shows a representative section from an animal receiving a plain NGC. Present within the conduit (upper left corner) and within the layer of $P4HB^+$ cells of the putative foreign body response (remainder of the image) are cells that appear to contain large vacuoles (arrows). Scale bars represent 100 μm in (A, B) and 20 μm in (C).

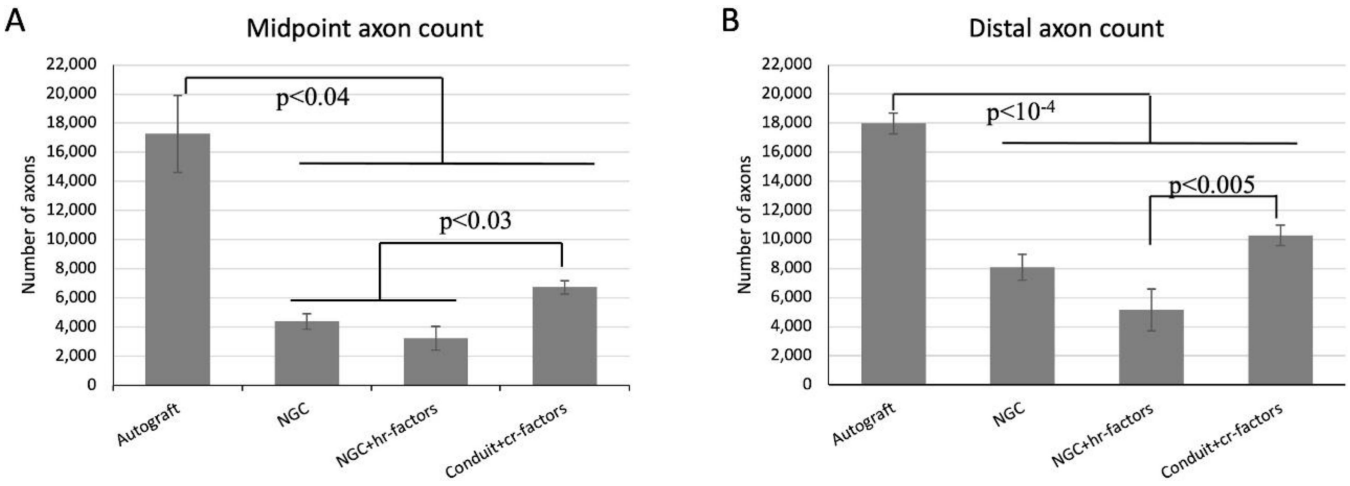

Figure 7.

Counts of myelinated axons. For animals where semi-thin sections were obtained, the number of myelinated axons in each graft or conduit was measured using stereology. The data are presented as mean ± standard error of the mean. (A) Counts of myelinated axon obtained from the midpoint of the autograft or NGCs. The number of myelinated axons was significantly higher in the autograft than in any of the NGCs ($p<0.04$). The axon counts were significantly higher in the NGC+cr-factors group than in the other two NGCs ($p<0.03$). (B) Counts of myelinated axon obtained from the distal nerve. The number of myelinated axons was again significantly higher in the autograft group than in any of the NGC groups ($p<10^{-4}$) and higher in the NGC+cr-factors group than in the NGC+hr-factors group ($p<0.005$).